



Safe Control Design for Unknown Nonlinear Systems with Koopman-based Fixed-Time Identification

Mitchell Black * Dimitra Panagou **

* Department of Aerospace Engineering, University of Michigan, Ann Arbor, MI 48109, USA (e-mail: mbblackjr@umich.edu).

** Department of Robotics and Department of Aerospace Engineering, University of Michigan, Ann Arbor, MI 48109, USA (e-mail: dpaganou@umich.edu)

Abstract: We consider the problem of safe control design for a class of nonlinear, control-affine systems subject to an unknown, additive, nonlinear disturbance. Leveraging recent advancements in the application of Koopman operator theory to the field of system identification and control, we introduce a novel fixed-time identification scheme for the infinitesimal generator of the infinite-dimensional, but notably linear, Koopman dynamical system analogous to the nonlinear system of interest. That is, we derive a parameter adaptation law that allows us to recover the unknown, residual nonlinear dynamics in the system within a finite-time, independent of an initial estimate. We then use properties of fixed-time stability to derive an estimation error bound on the unknown dynamics as an explicit function of time, which allows us to synthesize a safe controller using control barrier function based methods. We conduct a quadrotor-inspired case study in support of our proposed method, in which we show that safe trajectory tracking is achieved despite unknown, nonlinear dynamics.

Copyright © 2023 The Authors. This is an open access article under the CC BY-NC-ND license (<https://creativecommons.org/licenses/by-nc-nd/4.0/>)

Keywords: Control of constrained systems; identification for control; robust adaptive control; fixed-time stability; nonlinear system identification.

1. INTRODUCTION

Recent advances in computing power and memory storage have ushered in an era of estimation, identification, and control for autonomous systems dominated by data-driven methods. For example, compared to the 74 kilobytes of memory available on the United States National Aeronautics and Space Administration's (NASA) first lunar module computer, the gigabytes of memory used in many of today's data-driven approaches to dynamical system identification (e.g., deep neural networks) have allowed engineers to create significantly more expressive models. Though regression methods are widely-used for linear system identification, the field of identification for nonlinear systems is vast. Popular approaches in recent years include classes of neural networks (NNs), including deep NNs (e.g., Zancato and Chiuso (2021)) and recurrent NNs for time-varying systems (Gonzalez and Yu (2018)), Gaussian processes (Frigola and Rasmussen (2013)), and more recently the application of Koopman operator theory (e.g., Mauroy and Goncalves (2020); Brunton et al. (2016); Klus et al. (2020), among others), which introduces an infinite-dimensional but notably linear representation of a nonlinear system on which traditional linear identification approaches may be used.

Under Koopman theory, there exists a linear Koopman dynamical system that captures the dynamics of the original nonlinear system over an infinite-dimensional space of scalar functions known as observables. Beginning with

Mauroy and Goncalves (2020), recent work has focused on using data-driven approaches to approximate a finite-dimensional matrix representation of the Koopman operator, which acts as a state-transition operator for the Koopman dynamical system. In particular, extended dynamic mode decomposition (EDMD), first introduced in Williams et al. (2015) has emerged as a popular tool for carrying out such an approximation. The end result in many cases is a batched estimate of either the Koopman matrix (i.e., in Bruder et al. (2021); Haseli and Cortés (2021)) or its infinitesimal generator (Klus et al. (2020); Drmač et al. (2021)) obtained by solving a least-squares regression problem constructed from data. Potential shortcomings of this class of approaches include slower response times than e.g., recursive methods, and a lack of formal guarantees on the approximation error bound, which may be particularly detrimental when used in control design. In contrast, it has been shown by Black et al. (2022a) that fixed-time stability in the context of recursive parameter identification admits a such bound on the identification error as an explicit function of time.

Finite- and fixed-time stability (FTS and FxTS) are stronger notions of stability for equilibria of a dynamical system, each of which guarantees convergence of the system trajectories to the origin within a finite time. They have been used in the analysis of linear parameter identification schemes by Ríos et al. (2017); Ortega et al. (2022), and synthesized for the purpose of safe control design in Black et al. (2022a); Wang et al. (2022). One

benefit to recursive parameter identification in fixed-time, i.e., in a finite-time, independent of the initial condition, is the knowledge of an error bound on the identification error as an explicit function of time. When synthesized with a safe control law, this class of identification schemes yields less conservative control solutions, as highlighted in Black et al. (2022a).

Control barrier functions (CBFs) have proven to be a useful tool for safe control synthesis. As a model-based approach, however, it is critical that an accurate system model be available in order to preserve forward invariance of the set of safe states. Though robust CBF controllers can protect against bounded disturbances to the system dynamics (e.g., Jankovic (2018); Black et al. (2020)), the cost is conservatism. Various other approaches to safe control have sought to adapt to the unknown residual dynamics (e.g., Taylor and Ames (2020); Lopez et al. (2021)), or to learn their effects via data-driven Koopman-based policies both online (Folkestad et al. (2020)) and offline (Zinage and Bakolas (2022)). None of these methods, however, provide guarantees on learning convergence time.

In this paper, we address this open problem by introducing a Koopman-based identification scheme for safe control design that guarantees convergence within a fixed-time for a class of nonlinear, control-affine systems subject to an additive, nonlinear perturbation. We use knowledge of the bound on convergence time to quantify the identification error as an explicit function of time, the magnitude of which is leveraged to design a safe CBF-based controller. We demonstrate the advantages of our proposed approach on a trajectory tracking problem, and highlight that the identification and control laws succeed in preserving safety of the system even in the presence of measurement noise.

The rest of the paper is organized as follows. In Section 2, we introduce the preliminaries and define the problem under consideration. Section 3 contains our main result on fixed-time nonlinear system identification, which we use in Section 4 to design a safe controller. We demonstrate the approach on a numerical case study in Section 5, and conclude in Section 6 with directions for future work.

2. PRELIMINARIES AND PROBLEM STATEMENT

In this paper, we use the following notation. \mathbb{R} denotes the set of real numbers. The vector of size $n \times 1$ with all elements equal to one is denoted $\mathbf{1}_{n \times 1}$. We use $\|\cdot\|$ to denote the 2-norm and $\|\cdot\|_\infty$ to denote the supremum norm. We denote the minimum and maximum eigenvalue of a matrix \mathbf{M} as $\lambda_{\min}(\mathbf{M})$ and $\lambda_{\max}(\mathbf{M})$, and refer to its r^{th} singular value as $\sigma_r(\mathbf{M})$, to its nullspace as $\mathcal{N}(\mathbf{M})$, and its i^{th} column as $\text{col}_i(\mathbf{M})$. The gradient operator is ∇ , and the Lie derivative of a function $V : \mathbb{R}^n \mapsto \mathbb{R}$ along a vector field $f : \mathbb{R}^n \mapsto \mathbb{R}^n$ at a point $x \in \mathbb{R}^n$ is denoted as $L_f V(x) \triangleq \frac{\partial V}{\partial x} f(x)$.

Consider the following class of nonlinear, control-affine systems

$$\dot{\mathbf{x}} = f(\mathbf{x}(t)) + g(\mathbf{x}(t))\mathbf{u}(t) + d(\mathbf{x}(t)), \quad \mathbf{x}(0) = \mathbf{x}_0, \quad (1)$$

where $\mathbf{x} \in \mathcal{X} \subset \mathbb{R}^n$ and $\mathbf{u} \in \mathbb{R}^m$ denote the state and control input vectors, the drift vector field $f : \mathbb{R}^n \mapsto \mathbb{R}^n$ and control matrix field $g : \mathbb{R}^n \mapsto \mathbb{R}^n \times \mathbb{R}^m$ are known and continuous, and $d : \mathbb{R}^n \mapsto \mathbb{R}^n$ is an unknown disturbance

known to be continuous and to obey $\|d(\mathbf{x})\|_\infty \leq D < \infty$ for all $\mathbf{x} \in \mathcal{X}$. Consider also the following set of safe states,

$$\mathcal{S} = \{\mathbf{x} \in \mathcal{X} \mid h(\mathbf{x}) \geq 0\}, \quad (2)$$

for a continuously differentiable function $h : \mathbb{R}^n \mapsto \mathbb{R}$, where the boundary and interior of \mathcal{S} are $\partial\mathcal{S} = \{\mathbf{x} \in \mathbb{R}^n \mid h(\mathbf{x}) = 0\}$ and $\text{int}(\mathcal{S}) = \{\mathbf{x} \in \mathbb{R}^n \mid h(\mathbf{x}) > 0\}$ respectively. The trajectories of (1) are said to be *safe* if the set \mathcal{S} is *forward-invariant*, i.e., if $\mathbf{x}_0 \in \mathcal{S} \implies \mathbf{x}(t) \in \mathcal{S}, \forall t \geq 0$. The following lemma, known as Nagumo's Theorem, provides necessary and sufficient conditions such that \mathcal{S} is forward-invariant.

Lemma 1. (Blanchini (1999)) Suppose that $\mathbf{u}(t)$ is continuous such that the closed-loop trajectories of (1) are uniquely determined in forward-time. The set \mathcal{S} is forward-invariant if and only if

$$\dot{h} = \frac{\partial h(\mathbf{x})}{\partial \mathbf{x}} \dot{\mathbf{x}} \geq 0, \quad \forall \mathbf{x} \in \partial\mathcal{S}. \quad (3)$$

In recent years, control barrier functions have emerged as a viable approach for control design satisfying (3).

Definition 1. (Ames et al. (2017)) Given a set $\mathcal{S} \subseteq \mathcal{X} \subset \mathbb{R}^n$ defined by (2) for a continuously differentiable function $h : \mathbb{R}^n \mapsto \mathbb{R}$, the function h is a **control barrier function** (CBF) defined on the set \mathcal{X} if there exists a Lipschitz continuous class \mathcal{K}_∞ function $\alpha : \mathbb{R} \mapsto \mathbb{R}$ such that

$$\sup_{\mathbf{u} \in \mathbb{R}^m} \dot{h}(\mathbf{x}, \mathbf{u}) \geq -\alpha(h(\mathbf{x})), \quad (4)$$

for all $\mathbf{x} \in \mathcal{X}$.

We refer to (4) as the CBF condition, and observe that it constitutes sufficiency for the satisfaction of (3). As such, any continuous control law $\mathbf{u}(t)$ that 1) admits unique closed-loop trajectories of (1) in forward-time and 2) satisfies (4) renders the trajectories of (1) safe. For the system (1), the CBF condition is

$$\sup_{\mathbf{u} \in \mathbb{R}^m} [L_f h(\mathbf{x}) + L_g h(\mathbf{x}) \mathbf{u} + L_d h(\mathbf{x})] \geq -\alpha(h(\mathbf{x})),$$

where, without identification of $d(\mathbf{x})$, the precise value of $L_d h(\mathbf{x})$ is unknown. By $\|d(\mathbf{x})\|_\infty \leq D$, however, it is known that

$$-b_d \leq L_d h(\mathbf{x}) \leq b_d,$$

where $b_d = D \left| \frac{\partial h(\mathbf{x})}{\partial \mathbf{x}} \right| \mathbf{1}_{n \times 1}$. Under such circumstances, a robust-CBF may be used for safe control design.

Definition 2. (Jankovic (2018)) Given a set $\mathcal{S} \subseteq \mathcal{X} \subset \mathbb{R}^n$ defined by (2) for a continuously differentiable function $h : \mathbb{R}^n \mapsto \mathbb{R}$, the function h is a **robust control barrier function** (r-CBF) for the system (1) defined on the set \mathcal{X} if there exists a Lipschitz continuous class \mathcal{K}_∞ function $\alpha : \mathbb{R} \mapsto \mathbb{R}$ such that

$$\sup_{\mathbf{u} \in \mathbb{R}^m} [L_f h(\mathbf{x}) + L_g h(\mathbf{x}) \mathbf{u} - b_d] \geq -\alpha(h(\mathbf{x})), \quad (5)$$

for all $\mathbf{x} \in \mathcal{X}$.

Designing a controller to protect against the worst possible disturbance in perpetuity, however, may lead to poor performance, especially if D is large. Recent work (e.g., Lopez et al. (2021); Black et al. (2022a)) has shown that this may be mitigated by using an estimate of the unknown disturbance $\hat{d}(\mathbf{x})$. Thus, we define the vector field estimation error $\tilde{d}(\mathbf{x})$ as

$$\tilde{d}(\mathbf{x}) := d(\mathbf{x}) - \hat{d}(\mathbf{x}).$$

In Black et al. (2022a), it was shown under mild assumptions that if the uncertain vector field is parameter-affine, i.e., if

$$d(\mathbf{x}) = \Delta(\mathbf{x})\boldsymbol{\theta}^*,$$

for some known, continuous, bounded regressor matrix $\Delta : \mathcal{X} \mapsto \mathbb{R}^{n \times p}$ and unknown, static, polytopic parameters $\boldsymbol{\theta}^* \in \Theta \subset \mathbb{R}^p$, then the vector field estimation error may be driven to zero within a fixed time using parameter adaptation, i.e., $\|\Delta(\mathbf{x}(t))(\boldsymbol{\theta}^* - \hat{\boldsymbol{\theta}}(t))\| \mapsto 0$ as $t \mapsto T < \infty$ for parameter estimates $\hat{\boldsymbol{\theta}}(t)$, independent of $\hat{\boldsymbol{\theta}}(0)$. We now review the notion of fixed-time stability.

2.1 Fixed-Time Parameter Identification

Consider a nonlinear, autonomous system of the form

$$\dot{\mathbf{x}} = F(\mathbf{x}), \quad \mathbf{x}(0) = \mathbf{x}_0, \quad (6)$$

where $F : \mathbb{R}^n \mapsto \mathbb{R}^n$ is continuous such that (6) admits a unique solution for all $\mathbf{x}_0 \in \mathbb{R}^n$, the value of which at time t is denoted $\varphi_t(\mathbf{x}_0)$, and where $F(0) = 0$.

Definition 3. (Polyakov (2012)) The origin of (6) is fixed-time stable (FxTS) if it is stable in the sense of Lyapunov and any solution $\varphi_t(\mathbf{x}_0)$ of (6) reaches the origin within a finite time T independent of \mathbf{x}_0 , i.e., $\exists T < \infty$ such that $\varphi_t(\mathbf{x}_0) = 0$ for all $t \geq T, \forall \mathbf{x}_0 \in \mathbb{R}^n$.

In what follows, we review a fixed-time stable parameter adaptation law from the literature.

Theorem 1. (Black et al. (2022a)) Consider a perturbed dynamical system of the form (1). Suppose that the following hold:

- i) the unknown, additive dynamics are parameter-affine, i.e., $d(\mathbf{x}) = \Delta(\mathbf{x})\boldsymbol{\theta}^*$,
- ii) there exist a known matrix $\mathbf{M}(t) \in \mathbb{R}^{n \times p}$ and vector $\mathbf{v}(t) \in \mathbb{R}^n$ such that $\mathbf{M}(t)(\boldsymbol{\theta}^* - \hat{\boldsymbol{\theta}}(t)) = \mathbf{v}(t)$,
- iii) the nullspace of $\Delta(\mathbf{x}(t))$ is constant for all $t \leq T$, i.e., $\mathcal{N}(\Delta(\mathbf{x}(t))) = \mathcal{N}(\Delta(\mathbf{x}(0))), \forall t \leq T$, where

$$T = \frac{\mu\pi}{2k_V^2\sqrt{ab}}, \quad (7)$$

with $a, b > 0$, $\mu > 2$, $k_V = \varsigma\sqrt{2\lambda_{\max}(\mathbf{\Gamma})}$, for constant, positive-definite, gain matrix $\mathbf{\Gamma} \in \mathbb{R}^{p \times p}$ and $\varsigma = \min_{t \leq T} \sigma_r(\mathbf{M}(t))$.

Then, under the ensuing parameter adaptation law,

$$\dot{\boldsymbol{\theta}} = \mathbf{\Gamma}\mathbf{M}^\top \mathbf{v} \left(a\|\mathbf{v}\|^{\frac{2}{\mu}} + \frac{b}{\|\mathbf{v}\|^{\frac{2}{\mu}}} \right), \quad (8)$$

the estimated disturbance $\hat{d}(\mathbf{x}(t))$ converges to the true disturbance $d(\mathbf{x}(t))$ within fixed-time T , i.e., $\Delta(\mathbf{x}(t))\hat{\boldsymbol{\theta}}(t) \mapsto \Delta(\mathbf{x}(t))\boldsymbol{\theta}^*$ as $t \mapsto T$, and $\Delta(\mathbf{x}(t))\hat{\boldsymbol{\theta}}(t) = \Delta(\mathbf{x}(t))\boldsymbol{\theta}^*$ for all $t \geq T$, independent of $\hat{\boldsymbol{\theta}}(0)$.

Proof. See (Black et al., 2022a, Proof of Theorem 3).

Theorem 1 provides a framework for adapting parameter estimates $\hat{\boldsymbol{\theta}}$ such that an unknown disturbance of the form $d(\mathbf{x}) = \Delta(\mathbf{x})\boldsymbol{\theta}^*$ is learned within fixed-time. It requires idealized conditions, however, namely the availability of perfect measurements. While this is clearly limiting, the robustness to bounded measurement noise has been proven by Black et al. (2022a). Specifically, convergence to a

neighborhood of $\Delta(\mathbf{x}(t))\boldsymbol{\theta}^*$ is guaranteed by $\Delta(\mathbf{x}(t))\hat{\boldsymbol{\theta}}(t)$ in fixed-time. We omit this analysis due to space constraints, and refer the reader to Black et al. (2022a) for details. In reality, however, it is far more common for the unknown vector field $d(\mathbf{x})$ to be nonlinear, which to this point has precluded the use of (8) as a learning or adaptation strategy. By utilizing Koopman operator theory, however, we can transform the problem of identifying the nonlinear function d into a linear, albeit infinite-dimensional, identification problem, which with appropriate modifications permits the use of the above adaptation framework.

2.2 Koopman Operator based Identification

Koopman theory dictates that a nonlinear system of the form (6) has an analogous and notably linear representation in an infinite-dimensional Hilbert space \mathcal{Q} consisting of continuous, real-valued functions $q : \mathcal{X} \mapsto \mathbb{R}$ referred to as *observables*. The continuous-time Koopman dynamical system analogous to (6) is then described by

$$\dot{q} = \mathcal{L}q, \quad q \in \mathcal{Q}, \quad (9)$$

where \mathcal{L} denotes the infinitesimal generator of the linear semigroup of Koopman operators $\mathcal{U}^t : \mathcal{Q} \mapsto \mathcal{Q}$, i.e.,

$$\mathcal{L}q = \lim_{t \rightarrow 0} \frac{\mathcal{U}^t q - q}{t} = F \cdot \nabla q.$$

For tractability, however, many works (e.g., Bruder et al. (2021); Drmač et al. (2021), among others) derive matrix representations $\mathbf{U} \in \mathbb{R}^{N \times N}$ and $\mathbf{L} \in \mathbb{R}^{N \times N}$ of the respective finite-rank operators $\mathcal{U}_N^t = \Pi_N \mathcal{U}^t|_{\mathcal{Q}_N}$ and $\mathcal{L}_N = \Pi_N \mathcal{L}|_{\mathcal{Q}_N}$, where $\Pi_N : \mathcal{Q} \mapsto \mathcal{Q}_N$ is a projection operator onto the subspace $\mathcal{Q}_N \subset \mathcal{Q}$ (spanned by $N > n$ linearly independent basis functions $\{\psi_i : \mathcal{X} \mapsto \mathbb{R}\}_{i=1}^N$) and $\mathcal{O}|_{\mathcal{Q}_N}$ denotes the restriction of the operator \mathcal{O} to \mathcal{Q}_N . We refer the reader to Mauroy et al. (2020) for additional details, and instead highlight that in practice \mathbf{U} and \mathbf{L} are taken to be the respective solutions to

$$\psi^\top(\mathbf{x})\mathbf{U} = (\psi(\varphi_t(\mathbf{x})))^\top, \quad (10)$$

$$\mathbf{L}^\top \psi(\mathbf{x}) = \frac{\partial \psi(\mathbf{x})}{\partial \mathbf{x}} F(\mathbf{x}), \quad (11)$$

where $\psi(\mathbf{x}) = [\psi_1(\mathbf{x}) \dots \psi_N(\mathbf{x})]^\top \in \mathbb{R}^N$ and $\frac{\partial \psi(\mathbf{x})}{\partial \mathbf{x}} \in \mathbb{R}^{N \times n}$.

If \mathbf{L} can be identified directly (as in e.g., Klus et al. (2020)), the vector field F may be reconstructed by solving (11) for $F(\mathbf{x})$. When this is not possible, identification of \mathbf{U} may be used to reconstruct F after computing \mathbf{L} via

$$\mathbf{L} = \frac{1}{T_s} \log \mathbf{U}, \quad (12)$$

in the case of sampled data, where \log denotes the principal matrix logarithm and $T_s > 0$ is the sampling interval. We observe that both (10) and (11) describe linear systems of equations of the form $\mathbf{a}^\top \mathbf{X} = \mathbf{b}$, and thus \mathbf{X} (in this case \mathbf{U} or \mathbf{L}) can be identified using linear identification techniques such as the parameter identification law (8).

2.3 Problem Statement

Now, reconsider the unknown, control-affine, nonlinear system (1). Suppose that an estimate of its Koopman

generator matrix $\hat{\mathbf{L}}$ is available, and let the estimated unknown vector field $\hat{d}(\mathbf{x})$ then via (11) be the solution to

$$\hat{\mathbf{L}}^\top \psi(\mathbf{x}) = \frac{\partial \psi(\mathbf{x})}{\partial \mathbf{x}} (f(\mathbf{x}) + g(\mathbf{x})\mathbf{u} + \hat{d}(\mathbf{x})).$$

We assume that $\frac{\partial \psi(\mathbf{x})}{\partial \mathbf{x}}$ is full column rank, which may be satisfied by design (e.g., sinusoidal basis functions), and thus have that $\hat{d}(\mathbf{x}) \mapsto d(\mathbf{x})$ as $\hat{\mathbf{L}} \mapsto \mathbf{L}$ (which can also be satisfied if $\hat{\mathbf{U}} \mapsto \mathbf{U}$). Define the vectorized Koopman matrix and generator ($\boldsymbol{\mu}^*$ and $\boldsymbol{\lambda}^*$), and their estimates ($\hat{\boldsymbol{\mu}}$ and $\hat{\boldsymbol{\lambda}}$), as

$$\boldsymbol{\mu}^* := [\text{col}_1^\top(\mathbf{U}) \dots \text{col}_N^\top(\mathbf{U})]^\top, \quad (13)$$

$$\boldsymbol{\lambda}^* := [\text{col}_1^\top(\mathbf{L}) \dots \text{col}_N^\top(\mathbf{L})]^\top, \quad (14)$$

$$\hat{\boldsymbol{\mu}} := [\text{col}_1^\top(\hat{\mathbf{U}}) \dots \text{col}_N^\top(\hat{\mathbf{U}})]^\top, \quad (15)$$

$$\hat{\boldsymbol{\lambda}} := [\text{col}_1^\top(\hat{\mathbf{L}}) \dots \text{col}_N^\top(\hat{\mathbf{L}})]^\top, \quad (16)$$

and observe that for the system (1) the relations (10) and (11) are equivalent to

$$\Psi(\mathbf{x})\boldsymbol{\mu}^* = (\psi(\varphi_t(\mathbf{x})))^\top, \quad (17)$$

and

$$\Psi(\mathbf{x})\boldsymbol{\lambda}^* = \frac{\partial \psi(\mathbf{x})}{\partial \mathbf{x}} (f(\mathbf{x}) + g(\mathbf{x})\mathbf{u} + d(\mathbf{x})), \quad (18)$$

respectively, where

$$\Psi(\mathbf{x}) := \begin{bmatrix} \psi^\top(\mathbf{x}) & 0 & \dots & 0 \\ 0 & \psi^\top(\mathbf{x}) & \dots & 0 \\ \vdots & & \ddots & \vdots \\ 0 & \dots & 0 & \psi^\top(\mathbf{x}) \end{bmatrix} \in \mathbb{R}^{N \times N^2}. \quad (19)$$

Let the Koopman matrix and Koopman generator estimation errors respectively be denoted

$$\tilde{\boldsymbol{\mu}} = \boldsymbol{\mu}^* - \hat{\boldsymbol{\mu}},$$

$$\tilde{\boldsymbol{\lambda}} = \boldsymbol{\lambda}^* - \hat{\boldsymbol{\lambda}},$$

and observe that $\Psi(\mathbf{x})\tilde{\boldsymbol{\lambda}} = \Psi(\mathbf{x})\boldsymbol{\lambda}^*$ for all $\tilde{\boldsymbol{\lambda}} \in \mathcal{N}(\Psi(\mathbf{x}))$.

We are now ready to formally define the problem under consideration.

Problem 1. Consider a dynamical system of the form (1). Design adaptation and control laws, $\dot{\tilde{\boldsymbol{\lambda}}} = \eta(\mathbf{x}, \mathbf{u}, \tilde{\boldsymbol{\lambda}})$ and $\mathbf{u} = \kappa(\mathbf{x}, \tilde{\boldsymbol{\lambda}})$ respectively, such that

- (1) the Koopman generator error vector, $\tilde{\boldsymbol{\lambda}}$, is rendered fixed-time stable to the nullspace of $\Psi(\mathbf{x})$, i.e., $\tilde{\boldsymbol{\lambda}}(t) \mapsto \mathcal{N}(\Psi(\mathbf{x}))$ as $t \mapsto T$ and $\tilde{\boldsymbol{\lambda}}(t) \in \mathcal{N}(\Psi(\mathbf{x}))$ for all $t \geq T$, independent of $\tilde{\boldsymbol{\lambda}}(0)$, and
- (2) the system trajectories remain safe for all time, i.e., $\mathbf{x}(t) \in \mathcal{S}$, $\forall t \geq 0$.

In the ensuing section, we introduce our approach to solving the first element of Problem 1.

3. NONLINEAR ESTIMATION IN FIXED-TIME

In this section, we introduce our proposed adaptation law $\dot{\tilde{\boldsymbol{\lambda}}} = \eta(\mathbf{x}, \mathbf{u}, \tilde{\boldsymbol{\lambda}})$ for the fixed-time identification of the Koopman generator vector $\boldsymbol{\lambda}$, which allows us to identify the unknown vector field $d(\mathbf{x})$ in (1) within a fixed-time. Before introducing one of our main results, we require the following assumptions.

Assumption 1. The projection of the infinite-dimensional Koopman operator \mathcal{U}^t onto the finite-rank subspace \mathcal{Q}_N exactly describes the evolution of observables $q \in \mathcal{Q}$, i.e., $\mathcal{U}_N^t q = (\Pi_N \mathcal{U}^t) q$, for all $q \in \mathcal{Q}$.

Assumption 2. There exist scalars $s > 0$, $T > 0$ such that $\sigma_N(\Psi(\mathbf{x}(t))) \geq s$ for all $0 \leq t \leq T$, where $\Psi(\mathbf{x}(t))$ is given by (19).

The satisfaction of Assumption 1 depends on the choice of N (and thus on the basis functions ψ), and while generally this is an open problem, recent work has studied the existence of Koopman invariant subspaces (see e.g., Brunton et al. (2016)), i.e., subspaces $\mathcal{Q}_N \subset \mathcal{Q}$ over which Assumption 1 holds. For our numerical study in Section 5, we find that bases ψ constructed using monomials or sinusoids work well. The satisfaction of Assumption 2, which is needed for our proposed adaptation law and bounds the minimum non-zero singular value of Ψ , evidently depends on the choice of basis functions ψ_i . Note, however, that $\Psi(\mathbf{x}(t))$ is guaranteed to be full row-rank (which implies that $\sigma_N(\Psi(\mathbf{x}(t))) > 0$) provided that $\exists i \in [N]$ such that $\psi_i(\mathbf{x}(t)) \neq 0$. This can be guaranteed with an appropriate choice of bases, e.g., $\psi_1(\mathbf{x}(t)) = 1$.

Theorem 2. Suppose that Assumptions 1 and 2 hold, where

$$T = \frac{w\pi}{4s\lambda_{\max}(\mathbf{\Gamma})\sqrt{ab}}, \quad (20)$$

with $a, b > 0$, $w > 2$, and $\mathbf{\Gamma} \in \mathbb{R}^{N^2 \times N^2}$ a constant, positive-definite gain matrix. Then, under the ensuing adaptation law

$$\dot{\tilde{\boldsymbol{\lambda}}} = \mathbf{\Gamma}\Psi^\top(\mathbf{x})\boldsymbol{\nu}(\mathbf{x}, \tilde{\boldsymbol{\lambda}}) \left(a\|\boldsymbol{\nu}(\mathbf{x}, \tilde{\boldsymbol{\lambda}})\|^{2/w} + \frac{b}{\|\boldsymbol{\nu}(\mathbf{x}, \tilde{\boldsymbol{\lambda}})\|^{2/w}} \right), \quad (21)$$

the Koopman generator error vector $\tilde{\boldsymbol{\lambda}}$ is rendered FxTS to the nullspace of $\Psi(\mathbf{x})$, i.e., $\tilde{\boldsymbol{\lambda}}(t) \mapsto \mathcal{N}(\Psi(\mathbf{x}(t)))$ as $t \mapsto T$ and $\tilde{\boldsymbol{\lambda}}(t) \in \mathcal{N}(\Psi(\mathbf{x}))$ for all $t \geq T$, independent of $\tilde{\boldsymbol{\lambda}}(0)$, where

$$\boldsymbol{\nu}(\mathbf{x}, \tilde{\boldsymbol{\lambda}}) = \frac{\partial \psi(\mathbf{x})}{\partial \mathbf{x}} \dot{\mathbf{x}} - \Psi(\mathbf{x})\tilde{\boldsymbol{\lambda}}. \quad (22)$$

Proof. We first show that there exists a time-invariant Koopman generator vector $\boldsymbol{\lambda}(t) = \boldsymbol{\lambda}^*$, $\forall t \geq 0$, and then prove that under (21) the associated Koopman generator error vector $\tilde{\boldsymbol{\lambda}}$ is rendered FxTS to $\mathcal{N}(\Psi(\mathbf{x}))$.

First, under Assumption 1 it follows that there exists a finite-rank operator $\mathcal{L}_N : \mathcal{Q}_N \mapsto \mathcal{Q}_N$ such that the nonlinear dynamics of (1) may be represented by the following linear system in the space of observables:

$$\dot{q} = \mathcal{L}_N q, \quad q \in \mathcal{Q}.$$

Then, there exists a finite-dimensional matrix representation $\mathbf{L} \in \mathbb{R}^{N \times N}$ in a basis $\{\psi_i : \mathcal{X} \mapsto \mathbb{R}\}_{i=1}^N$ corresponding to the operator \mathcal{L}_N such that the relation (11) holds over the trajectories of (1). Thus, the Koopman generator matrix \mathbf{L} admits the (time-invariant) Koopman generator vector $\boldsymbol{\lambda}^*$ defined by (14).

Next, observe that (18) over the trajectories of (1) may be modified to obtain

$$\begin{aligned} \Psi(\mathbf{x})\boldsymbol{\lambda}^* - \Psi(\mathbf{x})\tilde{\boldsymbol{\lambda}} &= \frac{\partial \psi(\mathbf{x})}{\partial \mathbf{x}} \dot{\mathbf{x}} - \Psi(\mathbf{x})\tilde{\boldsymbol{\lambda}}, \\ \Psi(\mathbf{x})\tilde{\boldsymbol{\lambda}} &= \boldsymbol{\nu}(\mathbf{x}, \tilde{\boldsymbol{\lambda}}), \end{aligned}$$

where $\nu(\mathbf{x}, \hat{\lambda})$ is given by (22). Thus, we have that the premises of Theorem 1 are satisfied with $M = \Psi$ and $v = \nu$ and the adaptation law (21) takes the form of (8). Then, with Assumption 2 it follows directly from Theorem 1 that $\hat{\lambda}$ is rendered FxTS to $\mathcal{N}(\Psi(\mathbf{x}))$ with settling time given by (20). This completes the proof.

We note that while the above result requires perfect measurements, it is predicated on Theorem 1, which as stated previously has been proven to be robust to bounded measurement noise. In what follows, we show how the parameter adaptation law (21) results in learning the exact disturbance $d(\mathbf{x})$ to the system dynamics (1) within fixed-time.

Corollary 1. Consider the system (1). Suppose that the premises of Theorem 2 hold, and that the estimated Koopman vector $\hat{\lambda}$ is adapted according to (21). If the estimated disturbance $\hat{d}(\mathbf{x})$ is taken to be

$$\hat{d}(\mathbf{x}(t)) = \frac{\partial \psi(\mathbf{x}(t))^\dagger}{\partial \mathbf{x}} \Psi(\mathbf{x}(t)) \hat{\lambda}(t) - a(\mathbf{x}(t), \mathbf{u}(t)), \quad (23)$$

where $a(\mathbf{x}(t), \mathbf{u}(t)) = f(\mathbf{x}(t)) + g(\mathbf{x}(t))\mathbf{u}(t)$, then, the vector field estimation error $\tilde{d}(\mathbf{x}(t))$ is rendered FxTS to the origin and the estimated disturbance $\hat{d}(\mathbf{x}(t))$ converges to the true disturbance $d(\mathbf{x}(t))$ within a fixed-time T given by (20), i.e., $\tilde{d}(\mathbf{x}(t)) \mapsto 0$ and $\hat{d}(\mathbf{x}(t)) \mapsto d(\mathbf{x}(t))$ as $t \mapsto T$ independent of $\hat{d}(\mathbf{x}(0))$.

Proof. We first observe from (18) that the disturbance $d(\mathbf{x}(t))$ is the solution to

$$\frac{\partial \psi(\mathbf{x}(t))}{\partial \mathbf{x}} d(\mathbf{x}(t)) = \Psi(\mathbf{x}(t)) \lambda^* - \frac{\partial \psi(\mathbf{x}(t))}{\partial \mathbf{x}} a(\mathbf{x}(t), \mathbf{u}(t)). \quad (24)$$

Next, it follows from Theorem 2 that under (21) $\hat{\lambda}(t) \mapsto \lambda^*$ as $t \mapsto T$. Then, we have that $\Psi(\mathbf{x}(t)) \hat{\lambda}(t) \mapsto \Psi(\mathbf{x}(t)) \lambda^*$ and thus that $\frac{\partial \psi(\mathbf{x}(t))}{\partial \mathbf{x}} \hat{d}(\mathbf{x}(t)) \mapsto \frac{\partial \psi(\mathbf{x}(t))}{\partial \mathbf{x}} d(\mathbf{x}(t))$ as $t \mapsto T$ when $\hat{d}(\mathbf{x}(t))$ is taken to be the solution to (24). Finally, with $\frac{\partial \psi(\mathbf{x}(t))}{\partial \mathbf{x}}$ full column rank we use its pseudoinverse $\frac{\partial \psi(\mathbf{x}(t))^\dagger}{\partial \mathbf{x}}$ to recover (23) and thus have that $\hat{d}(\mathbf{x}(t)) \mapsto d(\mathbf{x}(t))$ as $t \mapsto T$.

For the purpose of control design, it is important to know how the estimation error signals behave during the transient period $t \leq T$ before the unknown vector field $d(\mathbf{x})$ has been learned. In contrast to least-squares and related regression-based approaches to learning the Koopman matrix U and/or generator matrix L , our FxTS parameter adaptation law allows us to derive explicit estimation error bounds as a function of time. In fact, prior work (see Black et al. (2022a)) has shown that the magnitude of this error bound is a monotonically decreasing function of time. In the following result, we introduce a modification to the prior work in order to derive a bound on the magnitude of the vector field estimation error $\tilde{d}(\mathbf{x}(t))$ as an explicit function of time.

Corollary 2. Suppose that the premises of Corollary 1 hold. If, in addition, the initial estimated Koopman generator vector is set to zero, i.e., $\hat{\lambda}(0) = \mathbf{0}_{N^2 \times 1}$, and Γ in (21) is constant, positive-definite, and also *diagonal*, then $\forall t \in [0, T]$, where T is given by (20), the following expression constitutes a monotonically decreasing upper bound on $\|\tilde{d}(\mathbf{x}(t))\|_\infty$:

$$\|\tilde{d}(\mathbf{x}(t))\|_\infty \leq \Lambda \sigma_{\max}(\mathbf{W}(t)) \tan^{\frac{w}{2}}(A(t)) := \delta(t), \quad (25)$$

where

$$\Lambda = \sqrt{2\lambda_{\max}(\Gamma)} \left(\frac{a}{b} \right)^{w/4}, \quad (26)$$

and

$$\mathbf{W}(t) = \frac{\partial \psi(\mathbf{x}(t))^\dagger}{\partial \mathbf{x}} \Psi(\mathbf{x}), \quad (27)$$

$$A(t) = \max \left\{ \Xi - \frac{\sqrt{ab}}{w} t, 0 \right\}, \quad (28)$$

$$\Xi = \tan^{-1} \left(\sqrt{\frac{b}{a}} \left(\frac{1}{2} \mathbf{l}^\top \Gamma^{-1} \mathbf{l} \right)^{\frac{1}{w}} \right), \quad (29)$$

where $\mathbf{l} = \frac{2D}{\sigma_{\min}(\mathbf{W}(0))} \cdot \mathbf{1}_{N^2 \times 1}$, and $\|\tilde{d}(\mathbf{x}(t))\|_\infty = 0, \forall t > T$.

Proof. Follows from (Black et al., 2022a, Corollary 1), and omitted due to space.

Knowledge of the upper bound on the disturbance estimation error bound (25) permits the use of robust, adaptive model-based control techniques. In particular, we will show in the next section how to synthesize a CBF-based controller that guarantees safety both before and after the transient phase $t \leq T$ during which the unknown disturbance $d(\mathbf{x})$ is learned, and in doing so address the second element of Problem 1.

4. ROBUST-ADAPTIVE CONTROL DESIGN

In this section, we describe two approaches to synthesizing the Koopman-based parameter adaptation law with a CBF-based control law for safe control under model uncertainty.

4.1 Robust-CBF Approach

In the first approach, we demonstrate how to apply robust-CBF principles to the design of a safe controller $\mathbf{u} = \kappa(\mathbf{x}, \hat{\lambda})$ when using the Koopman-based adaptation scheme (21).

Theorem 3. Consider a system of the form (1), a safe set S defined by (2) for a continuously differentiable function $h : \mathcal{X} \mapsto \mathbb{R}$, and suppose that the premises of Corollary 2 hold. Then, any control input \mathbf{u} satisfying

$$\sup_{\mathbf{u} \in \mathbb{R}^m} [L_f h(\mathbf{x}) + L_g h(\mathbf{x}) \mathbf{u} + L_{\hat{d}} h(\mathbf{x}) - b_d(t)] \geq -\alpha(h(\mathbf{x})) \quad (30)$$

renders the trajectories of (1) safe, where

$$b_d(t) = \left| \frac{\partial h}{\partial \mathbf{x}} \right| \delta(t) \cdot \mathbf{1}_{n \times 1}, \quad (31)$$

and $\delta(t)$ is given by (25).

Proof. Observe that over the trajectories of (1)

$$\begin{aligned} \dot{h} &= L_f h(\mathbf{x}) + L_g h(\mathbf{x}) \mathbf{u} + L_{\hat{d}} h(\mathbf{x}) \\ &= L_f h(\mathbf{x}) + L_g h(\mathbf{x}) \mathbf{u} + \frac{\partial h}{\partial \mathbf{x}} \hat{d}(\mathbf{x}) + \frac{\partial h}{\partial \mathbf{x}} \tilde{d}(\mathbf{x}) \\ &\geq L_f h(\mathbf{x}) + L_g h(\mathbf{x}) \mathbf{u} + \frac{\partial h}{\partial \mathbf{x}} \hat{d}(\mathbf{x}) - \left| \frac{\partial h}{\partial \mathbf{x}} \right| \delta(t) \cdot \mathbf{1}_{n \times 1}. \end{aligned}$$

By Corollary 2 it follows that $\|\tilde{d}(\mathbf{x}(t))\|_\infty \leq \delta(t)$ for all $t \geq 0$. Therefore, $\dot{h} \geq -\alpha(h(\mathbf{x}))$ whenever (30) holds, and

thus S is rendered forward-invariant by any control input satisfying (30).

It is worth noting that as the estimated disturbance $\hat{d}(\mathbf{x})$ converges to the true disturbance $d(\mathbf{x})$ the robustness term $b_d(t)$ will go to zero. So while initially the condition (30) may demand large control inputs to guarantee safety in the face of an unknown disturbance, as $t \mapsto T$ the term $b_d(t) \mapsto 0$ and the standard CBF condition is recovered.

4.2 Robust-Adaptive CBF Approach

In this approach, we define the following robust-adaptive safe set

$$\mathcal{S}_r = \{\mathbf{x} \in \mathcal{X} : h_r(\mathbf{x}, t) \geq 0\} \quad (32)$$

for the continuously differentiable function

$$h_r(\mathbf{x}, t) = h(\mathbf{x}) - \frac{1}{2}\delta^\top(t)\boldsymbol{\Omega}^{-1}\delta(t),$$

for $\delta(t) = \delta(t) \cdot \mathbf{1}_{n \times 1}$ with $\delta(t)$ given by (25), and a constant, positive-definite matrix $\boldsymbol{\Omega} \in \mathbb{R}^{n \times n}$. We note that the set \mathcal{S}_r defined by (32) is a subset of the safe set \mathcal{S} defined by (2), i.e., $\mathcal{S}_r \subseteq \mathcal{S}$. We now introduce a robust-adaptive CBF condition that renders the trajectories of (1) safe.

Theorem 4. Consider a system of the form (1), a set \mathcal{S}_r defined by (32) for a continuously differentiable function $h_r : \mathcal{X} \mapsto \mathbb{R}$, and suppose that the premises of Corollary 2 hold. Then, any control input \mathbf{u} satisfying

$$\sup_{\mathbf{u} \in \mathbb{R}^m} [L_f h_r(\mathbf{x}) + L_g h_r(\mathbf{x})\mathbf{u} - r(t, \hat{d}(\mathbf{x}(t)))] \geq -\alpha(h_r(\mathbf{x})) \quad (33)$$

renders the trajectories of (1) safe, where

$$r(t, \hat{d}(\mathbf{x}(t))) = \text{Tr}(\boldsymbol{\Omega}^{-1})\delta(t)\dot{\delta}(t) + b_d(t),$$

where $\delta(t)$ is given by (25), $b_d(t)$ is given by (31), and

$$\begin{aligned} \dot{\delta}(t) &= \Lambda\dot{\sigma}_{\max}(\mathbf{W}(t))\tan^{\frac{w}{2}}(A(t)) \\ &\quad - \frac{1}{2}\Lambda\sigma_{\max}(\mathbf{W}(t))\sqrt{ab}\tan^{\frac{w}{2}-1}(A(t))\sec^2(A(t)) \end{aligned} \quad (34)$$

Proof. Follows directly from (Black et al., 2022a, Theorem 5) by replacing $\tilde{\theta}$ with $\tilde{d}(\mathbf{x})$.

Remark 1. We note that the robust-adaptive CBF condition (33) requires the time-derivative of the maximum singular value of the matrix $\mathbf{W}(t)$ given by (27), i.e., $\dot{\sigma}_{\max}(\mathbf{W}(t))$. While this may not be available in closed-form, it may be approximated in practice using finite-difference methods.

Since both the robust (30) and robust-adaptive (33) CBF conditions ensure safety of the trajectories of (1), either condition may be included as an affine constraint in the now popular quadratic program based control law (eg. Ames et al. (2017); Black et al. (2020)). We now introduce one such iteration of the QP controller,

$$\begin{aligned} \mathbf{u}^* &= \arg \min_{\mathbf{u} \in \mathbb{R}^m} \frac{1}{2}\|\mathbf{u} - \mathbf{u}^0\|^2 \\ \text{s.t. } &\forall s \in [1..c] \end{aligned} \quad (35a)$$

$$\text{Either (30) or (33),} \quad (35b)$$

the objective (35a) of which seeks to find a minimally deviating solution \mathbf{u}^* from a nominal, potentially unsafe

input \mathbf{u}^0 subject to the specified CBF constraint (35b). In this way, the controller (35) may be used in conjunction with the adaptation law (8) for simultaneous system identification and control.

In the following section, we demonstrate the efficacy of our jointly proposed adaptation (21) and control (35) laws on a quadrotor tracking problem.

5. NUMERICAL CASE STUDY

Let \mathcal{F} be an inertial frame with a point s_0 denoting its origin. Consider a quadrotor seeking to track a Gerono lemniscate (i.e., figure-eight) trajectory amidst circular obstacles in the 2D plane. Quadrotor dynamics are known to be differentially flat, thus as shown to be feasible in Zhou and Schwager (2014) we take the model to be the following 2D double-integrator subject to an unknown, wind disturbance:

$$\begin{bmatrix} \dot{x} \\ \dot{y} \\ \dot{v}_x \\ \dot{v}_y \end{bmatrix} = \begin{bmatrix} v_x \\ v_y \\ a_x \\ a_y \end{bmatrix} + \begin{bmatrix} 0 \\ 0 \\ d_x(\mathbf{z}) \\ d_y(\mathbf{z}) \end{bmatrix}, \quad (36)$$

where x and y denote the position coordinates (in m), v_x and v_y are the velocities (in m/s), and a_x and a_y are the accelerations (in m/s²). The full state and control input vectors are $\mathbf{z} = [x \ y \ v_x \ v_y]^\top \in \mathbb{R}^4$ and $\mathbf{u} = [a_x \ a_y]^\top \in \mathbb{R}^2$ respectively, and $d_x : \mathbb{R}^4 \mapsto \mathbb{R}$ and $d_y : \mathbb{R}^4 \mapsto \mathbb{R}$ are unknown wind-gust accelerations satisfying the requirements of d in (1). Specifically, we used the wind-gust model from Davoudi et al. (2020) to obtain spatially varying wind velocities $w_i(\mathbf{z})$ and set $d_i(\mathbf{z}) = C_d(w_i(\mathbf{z}) - v_i)$ for $i \in \{x, y\}$, where C_d is a drag coefficient, such that $\|d_x(\mathbf{z})\|_\infty, \|d_y(\mathbf{z})\|_\infty \leq D = 10$.

We consider the presence of two circular obstacles, each of which occludes the desired quadrotor path. As such, the safe set is defined as

$\mathcal{S} = \{\mathbf{z} \in \mathbb{R}^4 : h_1(\mathbf{z}) \geq 0\} \cap \{\mathbf{z} \in \mathbb{R}^4 : h_2(\mathbf{z}) \geq 0\}$, where $h_i(\mathbf{z}) = (x - c_{x,i})^2 + (y - c_{y,i})^2 - R^2$ for $i \in \{1, 2\}$, $(c_{x,i}, c_{y,i})$ denotes the center of the i^{th} obstacle, and R is its radius. Since h_1, h_2 are relative-degree¹ two with respect to (36), we use future-focused CBFs for a form of safe, predictive control (see Black et al. (2022b) for details).

We use forms of the CBF-QP control law² (35) corresponding to both the robust (30) and robust-adaptive (33) CBF conditions, and compare the performance against a naive (i.e., assuming exact identification, $\hat{d} = d$) CBF controller equipped with the data-driven Koopman-based identification schemes proposed in Bruder et al. (2021) (which is denoted DD-KM and uses EDMD to learn the Koopman matrix from data) and Klus et al. (2020) (which is denoted DD-KG and uses EDMD to learn the Koopman generator from data) respectively, with each storing the last $N = 500$ measurements. For the robust and robust-adaptive simulations we inject additive noise sampled from $\mathcal{N}(0, 0.01)$ into both measurements of \mathbf{x} and $\dot{\mathbf{x}}$ in order to

¹ A function $p : \mathbb{R}^n \mapsto \mathbb{R}$ is said to be of relative-degree r with respect to the system dynamics if r is the number of times p must be differentiated before one of the control inputs appear explicitly.

² All simulation code and data are available online at <https://github.com/6lackmitchell/nonlinear-fxt-adaptation-control>

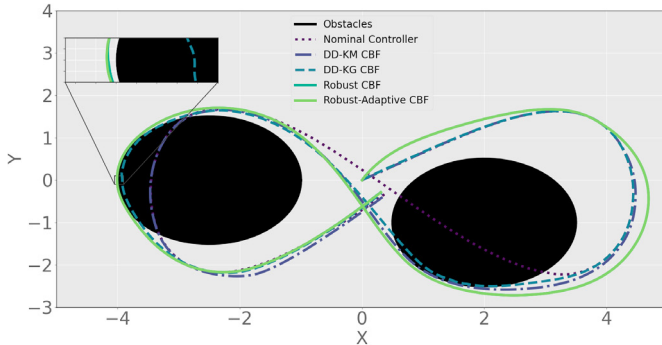


Fig. 1. XY paths under the various CBF-QP control laws in the double-integrator example. Only the controllers using the proposed Koopman-based fixed-time identification scheme succeed in preserving safety.

stress-test the algorithm under non-ideal conditions. We use the nominal control law introduced for quadrotors in Schoellig et al. (2012) and adapted for our dynamics, where the reference trajectory is the Gerono lemniscate defined by

$$\begin{aligned} x^*(t) &= 4 \sin(0.2\pi t) \\ y^*(t) &= 4 \sin(0.2\pi t) \cos(0.2\pi t), \end{aligned}$$

which specifies that one figure-eight pattern be completed every 10s. Our circular obstacles are centered on $(-2.5, 0)$ and $(2, -1)$ respectively, each with a radius of $R = 1.5\text{m}$. For all controllers, we used linear class \mathcal{K}_∞ functions $\alpha(h) = h$. For our Koopman basis functions, we used sinusoids of the form $\psi_i = \sqrt{2} \cos(n\pi z)$, $\psi_{i+1} = \sqrt{2} \sin(n\pi z)$, for $n \in \{1, 2\}$ and $z \in \{x, y, v_x, v_y\}$. We use a sampling time of $\Delta t = 0.001\text{s}$.

The resulting paths taken by the simulated CBF-controlled vehicles (Koopman-based naive, robust, and robust-adaptive), as well as the path taken for the nominally controlled vehicle without disturbance estimation are displayed in Figure 1. Here, only the robust and robust-adaptive CBF controllers that use our fixed-time identification approach preserve safety (as seen in Figure 2). As the data-driven Koopman matrix (Bruder et al. (2021)) and generator (Klus et al. (2020)) approaches are non-recursive and unable to quantify the identification error, they are neither sufficiently responsive nor accurate enough to guarantee safety in this example. Figure 3 highlights that our disturbance estimates indeed converge to the true values within the fixed-time $T = 0.12\text{ sec}$, computed using (20), and the control inputs are shown in Figure 4. We further note that even when measurement noise is injected into the system, the adaptation-based approach succeeds in both reconstructing the unknown disturbance to within a small error and preserving safety. We leave quantification of this measurement error and any error associated with representing the infinite-dimensional Koopman operator in a finite-dimensional subspace to future work.

6. CONCLUSION

We introduced a safe control synthesis using Koopman-based fixed-time system identification. We showed that under mild assumptions we can learn the unknown, additive, nonlinear vector field perturbing the system dynamics

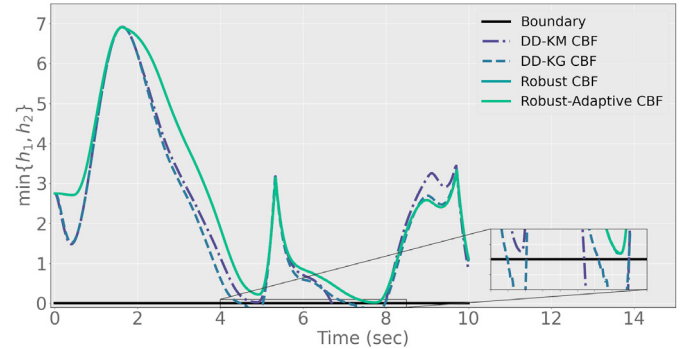


Fig. 2. Evolutions of h_1 and h_2 for the various controllers considered in the double-integrator example.

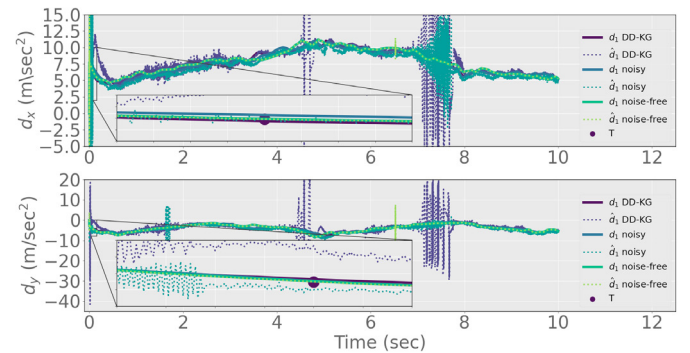


Fig. 3. The ground truths d_x , d_y and estimates \hat{d}_x , \hat{d}_y of the unknown wind gusts. In our scheme, the estimates converge to the true values within the fixed-time T without noise, and converge to a close approximation in the presence of measurement noise.

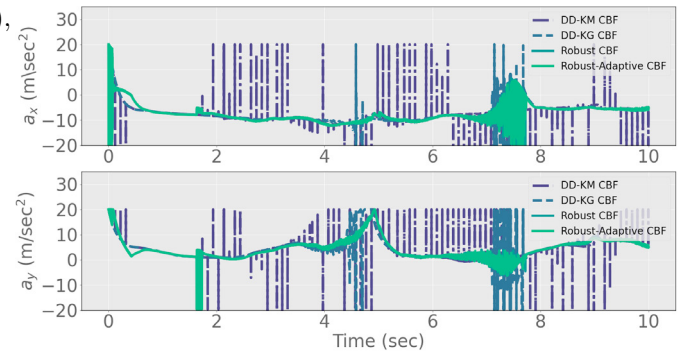


Fig. 4. Control inputs for the double-integrator example.

within a fixed-time independent of the initial estimate. The a priori knowledge of this identification guarantee allows us to derive robust and robust-adaptive control barrier function conditions suitable for use in a standard class of quadratic program-based controllers.

We recognize that there are practical limitations to our method, including the need to measure the state derivative and to be able to exactly represent the linear, infinite-dimensional Koopman dynamical system with a finite-rank operator. Though we demonstrated some robustness to measurement noise in our simulated study, in the future we will seek to relax these assumptions by analyzing the use of observers and filters for state and state-derivative

approximation and by seeking to quantify the residual error associated with projecting the infinite-dimensional Koopman operator onto a finite-dimensional subspace.

ACKNOWLEDGEMENTS

The authors would like to acknowledge the support of the National Science Foundation (NSF) through grants 1931982 and 1942907.

REFERENCES

Ames, A.D., Xu, X., Grizzle, J.W., and Tabuada, P. (2017). Control barrier function based quadratic programs for safety critical systems. *IEEE Trans. on Automatic Control*, 62(8), 3861–3876.

Black, M., Arabi, E., and Panagou, D. (2022a). Fixed-time parameter adaptation for safe control synthesis. *arXiv preprint arXiv:2204.10453*.

Black, M., Garg, K., and Panagou, D. (2020). A quadratic program based control synthesis under spatiotemporal constraints and non-vanishing disturbances. In *2020 59th IEEE Conference on Decision and Control (CDC)*, 2726–2731.

Black, M., Jankovic, M., Sharma, A., and Panagou, D. (2022b). Future-focused control barrier functions for autonomous vehicle control. *arXiv preprint arXiv:2204.00127*.

Blanchini, F. (1999). Set invariance in control. *Automatica*, 35(11), 1747–1767.

Bruder, D., Fu, X., Gillespie, R.B., Remy, C.D., and Vasudevan, R. (2021). Data-driven control of soft robots using koopman operator theory. *IEEE Transactions on Robotics*, 37(3), 948–961. doi:10.1109/TRO.2020.3038693.

Brunton, S.L., Brunton, B.W., Proctor, J.L., and Kutz, J.N. (2016). Koopman invariant subspaces and finite linear representations of nonlinear dynamical systems for control. *PLoS one*, 11(2), e0150171.

Davoudi, B., Taheri, E., Duraisamy, K., Jayaraman, B., and Kolmanovsky, I. (2020). Quad-rotor flight simulation in realistic atmospheric conditions. *AIAA Journal*, 58(5), 1992–2004.

Drmač, Z., Mezić, I., and Mohr, R. (2021). Identification of nonlinear systems using the infinitesimal generator of the koopman semigroup—a numerical implementation of the mauroy–goncalves method. *Mathematics*, 9(17), 2075. doi:10.3390/math9172075.

Folkestad, C., Chen, Y., Ames, A.D., and Burdick, J.W. (2020). Data-driven safety-critical control: Synthesizing control barrier functions with koopman operators. *IEEE Control Systems Letters*, 5(6), 2012–2017.

Frigola, R. and Rasmussen, C.E. (2013). Integrated pre-processing for bayesian nonlinear system identification with gaussian processes. In *52nd IEEE Conference on Decision and Control*, 5371–5376. IEEE.

Gonzalez, J. and Yu, W. (2018). Non-linear system modeling using lstm neural networks. *IFAC-PapersOnLine*, 51(13), 485–489.

Haseli, M. and Cortés, J. (2021). Data-driven approximation of koopman-invariant subspaces with tunable accuracy. In *2021 American Control Conference (ACC)*, 470–475. doi:10.23919/ACC50511.2021.9483259.

Jankovic, M. (2018). Robust control barrier functions for constrained stabilization of nonlinear systems. *Automatica*, 96, 359–367.

Klus, S., Nüske, F., Peitz, S., Niemann, J.H., Clementi, C., and Schütte, C. (2020). Data-driven approximation of the koopman generator: Model reduction, system identification, and control. *Physica D: Nonlinear Phenomena*, 406, 132416. doi:https://doi.org/10.1016/j.physd.2020.132416.

Lopez, B.T., Slotine, J.J.E., and How, J.P. (2021). Robust adaptive control barrier functions: An adaptive and data-driven approach to safety. *IEEE Control Systems Letters*, 5(3), 1031–1036. doi:10.1109/LCSYS.2020.3005923.

Mauroy, A. and Goncalves, J. (2020). Koopman-based lifting techniques for nonlinear systems identification. *IEEE Transactions on Automatic Control*, 65(6), 2550–2565. doi:10.1109/TAC.2019.2941433.

Mauroy, A., Susuki, Y., and Mezić, I. (2020). *Koopman operator in systems and control*. Springer.

Ortega, R., Bobtsov, A., and Nikolaev, N. (2022). Parameter identification with finite-convergence time alertness preservation. *IEEE Control Systems Letters*, 6, 205–210. doi:10.1109/LCSYS.2021.3057012.

Polyakov, A. (2012). Nonlinear feedback design for fixed-time stabilization of linear control systems. *IEEE Transactions on Automatic Control*, 57(8), 2106.

Ríos, H., Efimov, D., Moreno, J.A., Perruquetti, W., and Rueda-Escobedo, J.G. (2017). Time-varying parameter identification algorithms: Finite and fixed-time convergence. *IEEE Transactions on Automatic Control*, 62(7), 3671–3678.

Schoellig, A.P., Wiltsche, C., and D’Andrea, R. (2012). Feed-forward parameter identification for precise periodic quadrocopter motions. In *2012 American Control Conference (ACC)*, 4313–4318. doi:10.1109/ACC.2012.6315248.

Taylor, A.J. and Ames, A.D. (2020). Adaptive safety with control barrier functions. In *2020 American Control Conference (ACC)*, 1399–1405. doi:10.23919/ACC45564.2020.9147463.

Wang, S., Lyu, B., Wen, S., Shi, K., Zhu, S., and Huang, T. (2022). Robust adaptive safety-critical control for unknown systems with finite-time elementwise parameter estimation. *IEEE Transactions on Systems, Man, and Cybernetics: Systems*, 1–11. doi:10.1109/TSMC.2022.3203176.

Williams, M.O., Kevrekidis, I.G., and Rowley, C.W. (2015). A data-driven approximation of the koopman operator: Extending dynamic mode decomposition. *Journal of Nonlinear Science*, 25(6), 1307–1346.

Zancato, L. and Chiuso, A. (2021). A novel deep neural network architecture for non-linear system identification. *IFAC-PapersOnLine*, 54(7), 186–191.

Zhou, D. and Schwager, M. (2014). Vector field following for quadrotors using differential flatness. In *2014 IEEE International Conference on Robotics and Automation (ICRA)*, 6567–6572. doi:10.1109/ICRA.2014.6907828.

Zinage, V. and Bakolas, E. (2022). Neural koopman control barrier functions for safety-critical control of unknown nonlinear systems. *arXiv preprint arXiv:2209.07685*.